Nuclear Science and Techniques (2026) 37:5
https://doi.org/10.1007/s41365-025-01805-1

Evaluation of polycarbonate films as detection materials for high-dose electron beam radiation detection

Ke Wang[1,2] · Xiao-Dong Wang[1,2] · Xiong-Hui Fei[1,2]

Received: 16 July 2024 / Revised: 16 July 2024 / Accepted: 27 August 2024 / Published online: 6 December 2025

Abstract

In this study, the dosimetric characteristics (thickness applicability, preheating time, temperature and humidity dependence, in-batch uniformity, readout reproducibility, dose linearity, self-decay, and electron energy response) of engineered polycarbonate films irradiated with an electron beam (0–600 kGy) were investigated using photoluminescence spectroscopy. The results show a linear relationship between photoluminescence intensity and radiation dose when the thickness of the polycarbonate film is 0.3 mm. A higher fluorescence intensity can be obtained by preheating at 60 °C for 180 min before photoluminescence spectrum analysis. As the temperature during spectral testing and the ambient humidity (during and after irradiation) increased, the photoluminescence intensity of the polycarbonate films decreased. The photoluminescence intensity deviation of the polycarbonate films produced within the same batch at 100 kGy is 2.73%. After ten times of repeated excitations and readouts, the coefficients of variation in photoluminescence intensity are less than 8.6%, and the linear correlation coefficient between photoluminescence intensity and irradiation dose is 0.965 in the dose capture range of 20–600 kGy. Within 60 days of irradiation, the photoluminescence intensity of the polycarbonate film decreased to 60% of the initial value. The response of the 0.3 mm polycarbonate films to electron beams with energies exceeding 3.5 MeV does not differ significantly. This comprehensive analysis indicates the potential of polycarbonate films as a high-radiation dose detection material.

Keywords Electron beam irradiation · Polycarbonate · Dose detection · Radiophotoluminescence · Dosimetric characteristics

1 Introduction

In recent years, several types of thin-film polymer materials such as Gafchromic [1], clear Perspex [2], cellulose triacetate [3], and Sunna [4] have been listed as conventional radiation dosimeters according to the ISO/ASTM 51261(2002) standard. Compared with liquid or other types of dosimeters, organic-film dosimeters feature a low economic cost, stable fluorescence signal response, wide adaptability in shape and size, high detection dose limit, and wide dose detection range [5, 6]. They demonstrate significant potential in medical treatments, radiation processing control (such as food preservation and industrial material modification), nuclear track detection and visualization, dose monitoring at radiation sites, and decommissioning of nuclear facilities [5, 7–9].

However, the aforementioned film dosimeters present some disadvantages in the actual dose detection process, including low environmental adaptability, complex production processes, easy dose saturation, and short shelf life. Currently, studies pertaining to organic-film dosimeters focus primarily on two aspects. The first is investigation into new polymer films with favorable dose responses as

This work was supported by the National Natural Science Foundation of China (No. 12305385), Key Projects of Scientific Research of the Hunan Provincial Department of Education (22A0310), and the Research Startup Project of University of South China (220XQD025).

✉ Xiong-Hui Fei
fxh2021@usc.edu.cn

[1] School of Nuclear Science and Technology, University of South China, Hengyang 421001, China

[2] Key Laboratory of Advanced Nuclear Energy Design and Safety (MOE), University of South China, Hengyang 421001, China

alternative materials for dose detection, such as the development of new organic–inorganic composite materials. However, the processing of composite materials involves the issues of low material compatibility, complex manufacturing processes, unsatisfactory dose-response linearity, low durability, low long-term signal stability, rapid aging, low environmental adaptability, and high cost [10, 11]. The second the further analysis of the dosimetry characteristics of commercial or potential dosimeter materials, investigation into their applicable dosimetry scenarios, and proposal of schemes for structure optimization and performance improvement [12, 13]. Polycarbonate (PC) is a thermoplastic engineering plastic known for its excellent light transmission, impact resistance, ultraviolet-radiation resistance, high mechanical strength, and ease of processing [14]. They are widely utilized in industrial manufacturing, space science, electronic instruments, and medical devices [15]. Further investigations into the radiation effect of PC revealed that the aromatic ring structure in PC exhibited greater susceptibility to energy absorption and deposition compared with the aliphatic structure [16]. Irradiation can induce disorder in the internal structure of PC, thus resulting in intermolecular crosslinking (at 30 kGy), chain scission (at 200 kGy), and free radical generation [16–18]. Subsequent studies on the radiation modification of PC revealed its radiophotoluminescence properties [19, 20] and suggested PC as a promising material for radiation dose detection [21, 22]. During the initial period, relevant investigations on the radiation dose detection of PC films focused primarily on analyzing the measurable dose range, photoluminescence (PL) intensity, optimal excitation wavelength, fluorescence lifetime, optical quantum yield, light absorption, and transmission. However, few studies have investigated the dosimetry characteristics of PC films; therefore, PC films were primarily used for fluorescence-tracking detection in the early stages instead of dosimeters.

The dosimetric characteristics of PC films must be investigated before they can be used for practical dose detection [23]. These include considerations such as thickness applicability, preheating time, temperature and humidity dependence, dose rate response, dose linearity, in-batch uniformity, readout reproducibility, annealing, self-decay, and energy response. Soliman et al. investigated the PL spectra of different types of Makrofol PC materials (BL 95/8/2 6-2, DE 1-1, E, DE 1-4, KL 3-1005/1 6-2, DE 6-2, LT 6-4, and DE 7-2) irradiated with ^{60}Co-gamma rays (300 kGy) [24]. The findings revealed the distinct PL characteristics of each film, thereby enabling the application of different types of PC films in diverse scenarios based on their unique properties. Abdul-Kader et al. investigated a Makrofol LT 6-4 PC film irradiated with ^{60}Co-gamma rays and observed a decrease in the PL intensity with increasing irradiation dose within the range of 150–950 kGy and a linear correlation coefficient of 0.96 [25]. Posavec et al. reported that the PL intensity of irradiated PC films decreased with increasing temperature and that the ratio of PL peak intensity at 77–293 K ($I_{77\,K}I_{193\,K}$) was 1.93, thus demonstrating clear temperature dependence during testing [26]. Galante et al. discussed commercial PC detection films employed for monitoring radiation fields inside cylindrical container products. The correlation coefficient between the absorbed dose and response value was 0.99, thus indicating a favorable linear dose response [27]. Resta et al. irradiated Makrofol-KG PC films with $^{28}Si^{+}$ ions at 0.5, 1, and 2 MeV and discovered that the PL intensity of PC varied by two orders of magnitude at the same radiation dose of 1 and 2 MeV $^{28}Si^{+}$ ions, thus highlighting a significant difference in the energy response [28]. However, reports regarding the effects of PC thickness adaptability, preheating time before PL testing, and ambient humidity on dose detection, all of which can affect detection accuracy, are scarce. These factors have been considered in studies involving other types of dosimeters. Kattan et al. observed that polyvinyl-chloride films of varying thicknesses irradiated with 0–125 kGy gamma rays exhibited different degrees of radiation sensitivity [29]. Bhata et al. investigated a 250 µm- diethyl terephthalate film (also known as Garfilm-EM) irradiated with equal doses of ^{60}Co-gamma rays under various relative humidity (RH) conditions and discovered that the net absorbance of the film remained stable after 14 days, except for a rapid decline on the first day, thus indicating that the dose response of this film was affected by humidity during irradiation [30]. Mejri et al. discussed a commercial inorganic glass dose tablet exposed to different RH environments after γ-irradiation; the net absorbance of the dose tablet showed a distinct trend of reverse proportional decline within 22 days, thereby indicating a significant humidity response during storage after irradiation [31]. In summary, only a few dosimetric characteristics have been briefly mentioned in existing studies pertaining to the detection performance of various types of PC films, and an overall discussion on a specific PC film has not been provided.

In this study, PL spectroscopy was employed to investigate the dosimetric characteristics of engineered PC films after electron beam (EB) irradiation (0–600 kGy). The effects of the PC film thickness, PC preheating time after irradiation, temperature during PL spectrum test, ambient humidity during irradiation, and ambient humidity of the PC storage environment after irradiation on the PL spectral intensity were investigated. Additionally, the in-batch uniformity, readout reproducibility, dose linearity, PL intensity attenuation characteristics of the PC after irradiation, and PC response to different EB energies were investigated. This study aims to provide more detailed data indicators and analysis results for each dosimetric characteristic point, comprehensively evaluate the possibility of using PC films as a dosimeter in practical radiation detection, and provide

references for dosimetry studies involving other types of PC materials.

2 Materials and methods

2.1 Sample preparation

The PC film used in this study was fabricated by Covestro Polymer Co., Ltd., Shanghai, China. It is a nontoxic, odorless, colorless, and transparent glassy amorphous organic polymer [32]. The film exhibited a density of 1.25 g/cm^3, a light transmittance of 90% ±1%, a refraction index of 1.585 ±0.001, a linear expansion rate of 3.8×10^{-5} cm/°C, and a thermal deformation temperature of 140 °C. PC films of various thicknesses, i.e., 0.2, 0.3, 0.5, 0.8, 1.0, 1.5, and 2.0 mm, were prepared. The surface of the PC film was flat and the thickness was uniform. The films were cut into 20 mm × 20 mm squares, and the protective layers were removed from both sides for further use.

2.2 EB irradiation

Electron accelerators with different energies (3.5, 4, 4.5, 10, and 20 MeV) were used for PC irradiation in this study. A DD-type electron accelerator (Jinwo Technology Co., Ltd., CGN, China) operating in an energy range (EB) of 3.5–5 MeV and a beam power range of 30–200 kW was used. Additionally, an IS1020 backwave electron linear accelerator (Xianghua Huada Biotechnology Co., Ltd., Hunan, China) operating at an energy (EB) of 10 MeV and a rated beam power of 20 kW was used. The IS1020 high-energy electron accelerator (Huada Biotechnology Co., Ltd., Guangzhou, China) was also operated at an energy (EB) of 20 MeV and a maximum beam power of 20 kW. The PC film was placed on a conveyor belt and passed through the central area of the irradiation window multiple times to receive the required dose, with a single dose of 10 kGy per pass. Irradiation was performed at room temperature, and the radiation dose was traced using dichromate. The sample was uniformly irradiated using an EB with a dose deviation of 1%.

2.3 PL spectrum

An FLS1000 steady-state/transient fluorescence spectrometer (including conventional and variable temperature types) manufactured by the Edinburgh company, UK, was used to analyze the PL spectra of the irradiated PCs. The conventional type was operated under the following parameters: excitation spectrum scanning wavelength range, 250–450 nm; emission spectrum scanning wavelength range, 340–800 nm; scanning rate, 5°/min; step size, 1 nm; and integration time, 0.2 s. A xenon lamp was used as its excitation source, and the test was performed at ambient temperature. The variable-temperature type featured a built-in variable-temperature component (the Oxford Optistat thermostat) with an optional temperature range of 273–373 K and an insulation accuracy of ±1 K. The emission-spectrum scanning wavelength range was 395–800 nm, and the other parameters were set based on the conventional type. The irradiated PC film was placed at the same position on the PL spectrum test platform to ensure the consistency of the PL measurement path.

2.4 Analysis of dosimetric characteristics

2.4.1 Thickness applicability

A typical feature of thin-film dosimeters is their availability at different thicknesses [29]. To evaluate the response of PC films with different thicknesses to EB irradiation, seven groups of PC films with different thicknesses (0.2, 0.3, 0.5, 0.8, 1.0, 1.5, and 2.0 mm) were prepared. Each group of films was irradiated with different doses (0, 100, 300, and 600 kGy) under a 10 MeV EB, and irradiation treatment was performed at ambient temperature in an air atmosphere. Subsequently, the PL intensity was analyzed, and the relationship between the PL peak intensity and irradiation dose of the PC films with different thicknesses was obtained through PL spectral testing at the same ambient temperature.

2.4.2 Preheating time

Generally, the non-luminous center effect occurs in irradiated polymer films. When the irradiated PC film is preheated prior to the PL test, its PL intensity changes accordingly. Therefore, the optimal preheating conditions for irradiated PC films must be determined to achieve higher PL intensity values. In this study, eight groups (three parallel samples in each group) of 0.3 mm PC films were irradiated at 100 kGy by a10 MeV EB at ambient temperature in an air atmosphere and then preheated at 60 °C for 10, 30, 40, 60, 90, 120, 180, and 300 min, separately. Finally, the PL peak intensities of the PC films preheated for different durations were measured.

2.4.3 Temperature dependence

Temperature dependence refers to the effect of ambient temperature on the PL intensity of the PC film during PL spectrum testing [33]. To investigate the relationship between them, 0.3 mm PC films were irradiated at 100 kGy using a 10 MeV EB, and three parallel samples were prepared. PL tests were conducted at eight temperature points, i.e., 273, 278, 283, 293, 303, 323, 343, and 373 K. The variation in

the PL intensity with the ambient temperature during the PL test was analyzed.

2.4.4 Humidity dependence

The humidity of the environment affects the dose response of polymer films. Therefore, the effect of RH in air (both during irradiation and post-irradiation storage) on the PL intensity of the PC film was evaluated in this study [30, 31]. To establish different RH gradients in the range of 12.4–97.2%, various saturated salt solutions were prepared using the techniques reported by Wexler and Hasegawa (1954) and Levine (1979). Table 1 lists the types of saturated salt solutions selected and their corresponding RH values under sealed conditions. The corresponding saturated salt solution (25 ml) was added to a borosilicate glass bottle to establish a different humidity gradient.

In the study of humidity dependence during irradiation, the 0.3 mm PC film was suspended in sealed glass bottles in different humidity environments (12.4, 33.6, 54.9, 75.5, and 97.2%) and stored at room temperature for seven days to balance the ambient humidity of the PC film. Subsequently, the glass bottles were irradiated at 100 kGy using a 10 MeV EB, after which the five groups of PC films were subjected to PL tests. In the study of humidity dependence during storage after irradiation, each group of PC films was first irradiated using a 10 MeV EB (100 kGy) and then encapsulated in bottles under different humidity conditions for seven days under environmental regulation. Finally, PL tests were performed and the effect of humidity on the PL intensity of the PC films was analyzed.

2.4.5 In-batch uniformity

In-batch uniformity refers to the PL intensity uniformity of PC films produced in the same batch under the same irradiation dose. It is a key index for describing the dosimetric characteristics of RPL materials [34]. Three groups of 0.3 mm PC films (15 parallel samples per group) were irradiated (10 MeV EB) at 100, 300, and 600 kGy, separately. Irradiation treatment was performed at ambient temperature in an air atmosphere. The PL peak intensity of each sample was measured. The relative mean deviation (*RAD*), as expressed in Eq. (1) was used to evaluate the degree of uniformity in the PL intensity.

$$RAD = \frac{\sum_{i=1}^{n} |x_i - \bar{x}|}{n \times \bar{x}} \times 100\%, \quad (1)$$

where x_i denotes the measured value, $\bar{x}$ the average value, and n the number of parallel samples in the same dose group. After recording the PL peak intensities of the parallel samples in each dose group, the *RAD* value was obtained to analyze the in-batch uniformity of the PC irradiated film.

Table 1 Different types of saturated salt solutions and the corresponding humidity

Salt solution type	Relative humidity (%)
$LiCl \cdot H_2O$	12.4
$MgCl_2 \cdot 6H_2O$	33.6
$Mg(NO_3)_2 \cdot 6H_2O$	54.9
NaCl	75.5
K_2SO_4	97.2

2.4.6 Readout reproducibility

To investigate whether multiple PL tests affect the dose information stored in the PC film, three groups of 0.3 mm PC films were irradiated (10 MeV EB) at 100, 300, and 600 kGy, separately. Irradiation treatment was performed at ambient temperature in an air atmosphere. Each film was excited repeatedly and measured 10 times to obtain the PL peak intensity. To assess the dispersion of PL intensity, the coefficient of variation was estimated using Eq. (2).

$$C_v = \frac{\sigma}{\bar{x}} \times 100\%, \quad (2)$$

where C_v is the coefficient of variation, σ the standard deviation of the 10 measurements, and $\bar{x}$ the average value. Obtaining the standard deviation and coefficient of variation allowed for the evaluation of the readout reproducibility of the PC films.

2.4.7 Dose linearity

The dose linearity, which refers to the linear relationship between the measured signal intensity and the radiation dose, is a crucial parameter in dose detection [35]. In this study, the 0.3 mm PC films were irradiated with different doses (0, 20, 50, 100, 200, 400, and 600 kGy) using a 10 MeV EB (irradiation treatment was performed at ambient temperature in an air atmosphere). The relationship between the irradiation dose and PL intensity of the PC films after irradiation was analyzed via PL spectrum tests, and the dose capture range of the PC film was determined. The correlation coefficient (R^2) was used as a statistical indicator to reflect the degree of linear correlation.

2.4.8 Self-decay

Self-decay refers to a process in which the signal intensity of an irradiated sample declines with time [36]. To analyze the change in the PL peak intensity of the irradiated PC film after a certain duration, the 0.3 mm PC film was irradiated

(10 MeV EB) at 300 kGy (irradiation treatment was performed at ambient temperature in an air atmosphere) and then stored in a dark and dust-free area. The PL intensities of the PC films were measured on days 0, 1, 3, 5, 10, 20, 30, and 60 after irradiation. The decay characteristic curve was obtained by performing an appropriate function fitting.

2.4.9 Electron energy response

Electron energy response refers to the difference in the PL peak intensity when the PC films are irradiated with the same dose under different EB energies and is typically depicted as the relationship between the PL intensity and energy [37]. In this study, five EB energies (3.5, 4, 4.5, 10, and 20 MeV) were selected to irradiate 0.3 mm PC films at a dose of 100 kGy. Irradiation was performed in an air atmosphere at room temperature. The PL peak intensity of the PC film irradiated with a 10 MeV EB was used as a normalized basis to calculate the deviation in the PL peak intensity of PC films irradiated with EBs of other energy levels. (Positive and negative deviations were used, where values higher and lower than the reference value were positive and negative values, respectively.)

3 Results and discussion

The color of the PC film transformed to yellow and darkened gradually as the irradiation dose increased. This yellowing is associated with the formation of color centers during irradiation, such as phenoxyl and phenyl radicals. Radiation induces an increase in the internal structural disorder of PC, thereby creating conditions conducive to the formation of color centers [38]. However, the fading of the irradiated samples left for a certain duration is attributable to the oxygen reaction of free radicals within the PC film [39]. Based on excitation spectra tests, the optimal excitation wavelength of the PL spectrum for the PC film was determined to be 320 nm.

3.1 Thickness applicability

The variation in the mean value of the PL peak intensity detected by PC films of different thicknesses with the irradiation dose is shown in Fig. 1. The results show that the PL intensity of PC films with a thickness greater than or equal to 0.3 mm decreased as the dose increased, whereas the PL intensity of PC films with a thickness of 0.2 mm showed the opposite trend as the dose increased. The color of the PC film with the same thickness darkened as the irradiation dose increased. At the same irradiation dose, the color of the PC films darkened as the film thickness increased. The darker the color of the PC film, the greater was the

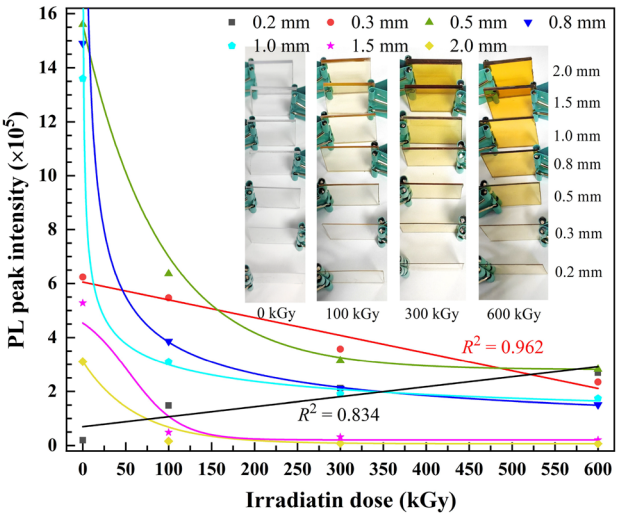

Fig. 1 (Color online) PL peak intensity of PC films with different thickness varying with irradiation dose

internal radiation damage. When the thickness of the PC film exceeded 0.5 mm, the PL peak intensity of the PC film treated with the same irradiation dose decreased as the thickness increased. The thicker the PC film, the higher was the deposited energy under the same irradiation dose, thus facilitating the formation of a two-layer structure composed of a top carbonization layer and a bottom cross-linked layer [40]. The formed carbonization layer affected the transmission of excitation and emission light in the PL spectral test.

As shown in the fitting curve, only the PL intensities of the 0.3 mm and 0.2 mm PC films were linearly related to the irradiation dose (0–600 kGy), and their linear correlation coefficients were 0.962 and 0.834, respectively. However, the 0.2 mm PC film exhibited low mechanical strength (which implies its susceptibility to mechanical damage and deformation), low dose linear response values (i.e., it may not be able to absorb sufficient radiation energy, thus resulting in inaccurate measurement results), and dose saturation tendencies. Therefore, a 0.3 mm-thick PC film was selected as the analysis sample in this study, thus aligning with the thickness of existing organic- film dose detection materials such as low-density polyethylene films (0.3 mm) [41] and Indian Garfilm-EM films (0.25 mm) [30].

3.2 Preheating time

Figure 2 shows the PL emission spectrum of the irradiated (100 kGy) PC film after being preheated at 60 °C for various durations. In the preheating-time range of 0–300 min, the PL peak intensity of the PC film initially increased and then decreased as the preheating time increased, with the maximum reached at approximately 180 min. As shown in the upper-right corner of Fig. 2, the PL peak intensity at 10, 30,

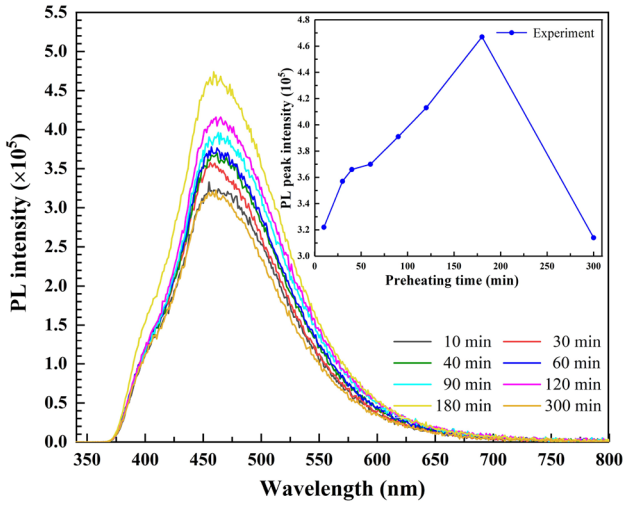

Fig. 2 (Color online) PL spectra of irradiated PC film treated with different preheating times at 60 °C

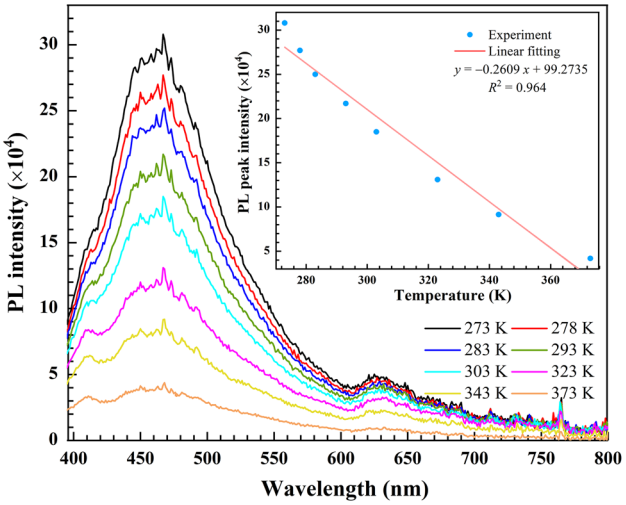

Fig. 3 (Color online) PL intensity curve of irradiated PC film at different ambient temperatures during PL spectrum testing

40, 60, 90, 120, and 300 min represent 68.9%, 76.4%, 78.4%, 79.2%, 83.7%, 88.4%, and 67.2% of the PL peak intensity at 180 min, respectively. The initial increase in the PL peak intensity is attributable to secondary electrons inside the PC film after irradiation being captured by non-luminescent centers. These electrons escape after absorbing heat energy and are recaptured by the luminous center. However, when the preheating time exceeds 180 min, the fluorescence signal of the PC film is quenched by heat more easily, thus resulting in a decrease in the fluorescence intensity. These results suggest that the PL intensity of the PC film can reach saturation after preheating for a certain period and that the optimal preheating time at 60 °C is 180 min. Based on existing literature, such as the optimal preheating condition for silver-doped inorganic glass RPL dosimeters being 40 min at 90 °C [42], future studies may investigate the possibility of reducing the preheating time by appropriately increasing the preheating temperature.

3.3 Temperature dependence

After irradiation, the PL spectra of the PC films were recorded at various ambient temperatures. The variations in the PL spectra of the irradiated (100 kGy) PC films at different ambient temperatures are shown in Fig. 3. The emission spectrum peak of the PC film was located at 470 nm. Additionally, a weak peak at 410 nm emerged and disappeared upon excitation with 350 nm UV light, thus indicating that it was the scattering peak of the sample. Within the temperature range of 273–373 K, the PL intensity decreased as the ambient temperature increased. The PL peak intensity at 373 K decreased to 13.3% of its initial intensity at 273 K, and this decreasing trend is consistent with the effect of temperature on the PL intensity of fluorescent materials [26]. This may result from the inhibition of non-radiative recombination processes at low temperatures [43], with fluorescence thermal quenching occurring as the temperature increases, thus resulting in a reduced PL intensity [44]. The relationship between PL peak intensity and temperature is shown in the upper-right illustration in Fig. 3. They exhibit a relationship expressed by $y = -0.2609\,x + 99.2735$ (where y is the PL peak intensity and x is the ambient temperature), with a correlation coefficient of 0.964. These results indicate that the PC film maintained a favorable temperature-dependent linear relationship within the range of 273–373 K, thus suggesting its utility as a temperature sensor in future applications.

3.4 Humidity dependence

The effects of the ambient humidity on the PL intensity of the PC film during and after irradiation are shown in Fig. 4a, b, respectively. A comparison of the results shown in the two figures above shows that the PL intensity of the PC film decreased as the RH increased (during irradiation and post-irradiation storage), whereas the peak position remained unchanged. However, when the ambient humidity increased from 12.4 to 97.2% during irradiation, the PL peak intensity of the PC film decreased to 74.3% of the initial value, whereas when the ambient humidity increased from 12.4 to 97.2% after irradiation, the PL peak intensity of PC film decreased to 53.3% of the initial value. Thus, one can conclude that the effect of the storage environment humidity on the PL intensity of the PC film after irradiation is more significant compared with the case during irradiation, and that the PL response value of the PC film decreases with an

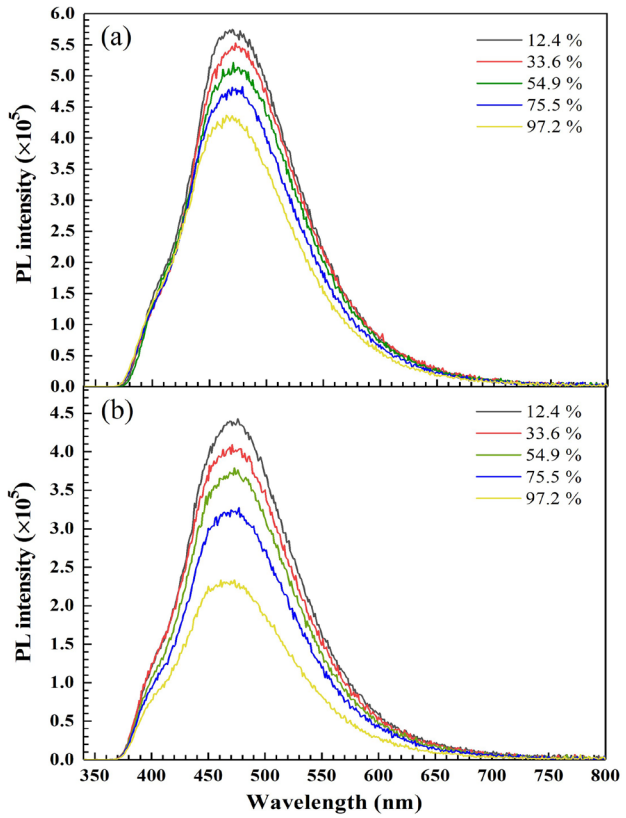

Fig. 4 (Color online) PL spectra of irradiated PC films under different RH conditions: **a** during irradiation; **b** during storage after irradiation

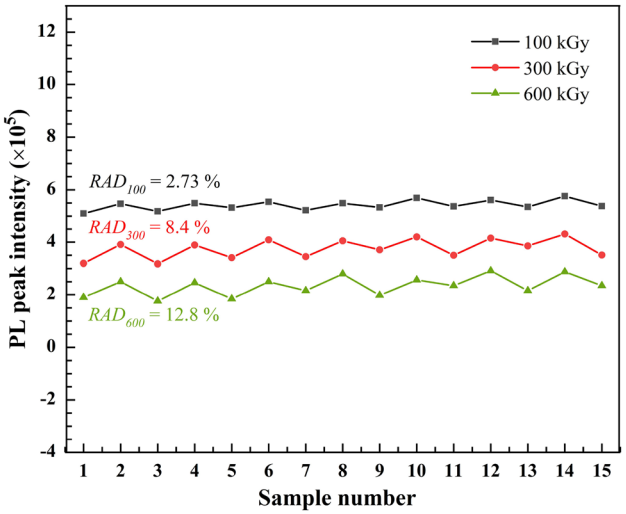

Fig. 5 (Color online) Variation in PL peak intensity among different PC films produced within the same batch under same dose irradiation

increase in the ambient humidity. This phenomenon is attributable to the radiation, which generated the corresponding free radical sites on the PC main chain. Moreover, the interaction between the radiation and water molecules generates free radicals and active particles, which can interact with the PC film. Therefore, the increase in environmental humidity during irradiation generates more free radicals, which further interact with the PC film. The increase in humidity in the storage environment after irradiation accelerates the diffusion of oxygen into the PC matrix and further oxidizes the PC, thus reducing the PL intensity [30]. The humidity dependence results of the PC films are similar to those of FWT, Mylar, Melinex, and PET film dosimeters [45–49]. Further discussion is warranted regarding the declining trend of PL intensity over time under different ambient humidities.

3.5 In-batch uniformity

The PL peak intensities detected for the different PC films produced in the same batch after the irradiation under the same dose are shown in Fig. 5. At radiation doses of 100, 300, and 600 kGy, the variation ranges of the PL peak intensity counts were $5.1 \times 10^5 - 5.76 \times 10^5$, $3.18 \times 10^5 - 4.2 \times 10^5$, and $1.76 \times 10^5 - 2.92 \times 10^5$, respectively. As the irradiation dose increased from 100 to 600 kGy, the fluctuation range of the PL peak intensity increased. The relative average deviation corresponding to the three doses were 2.73%, 8.4%, and 12.8%, respectively. These results show that the in-batch uniformity of the PC film under doses less than 100 kGy is ideal and that the signal uniformity is similar to that of a GD-300 dosimeter (the deviation values of GD-300 at doses of 0.2, 20, and 200 mGy are ±1.7%, ±1.3%, and ±1.1%, respectively) [24, 42]. However, when the dose exceeded 100 kGy, the relative average deviation of the in-batch uniformity of the PC film increased, and its effect on the dose detection accuracy should be considered [50].

3.6 Readout reproducibility

Under three different radiation doses, the PC film was repeatedly excited and measured 10 times; the corresponding PL peak intensity values are shown in Fig. 6. The results show that the variation ranges of the PL peak intensity counts at irradiation doses of 100, 300, and 600 kGy were $5.04 \times 10^5 - 5.56 \times 10^5$, $3.54 \times 10^5 - 3.7 \times 10^5$, and $2.16 \times 10^5 - 2.81 \times 10^5$, respectively, while the mean values of the PL peak intensity counts were 5.277×10^5, 3.616×10^5, and 2.547×10^5, respectively. The dose response is consistent with the data shown in Fig. 5. Additionally, the standard deviations of the three data groups were 0.158, 0.044, and 0.23, respectively, and the coefficients of variation of the PL intensity values were calculated to be between 1.2% and 8.6%. Compared with the GD-351 dosimeter (whose coefficient of variation for readout reproducibility in the dose range of 0.2–200 mGy is 15–19%) [42], the PC film exhibited a smaller standard deviation and

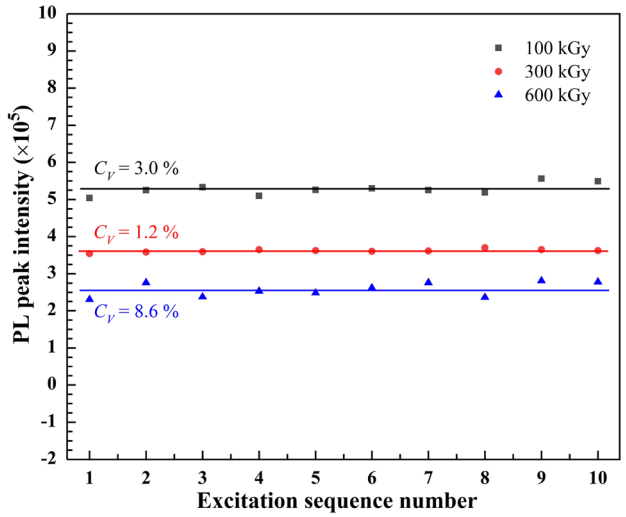

Fig. 6 (Color online) PL peak intensity of irradiated PC film obtained after 10 times of repeated excitation and readout

coefficient of variation. This indicates the favorable readout reproducibility of the irradiated PC film.

3.7 Dose linearity

The PL emission spectra of the PC films irradiated at different doses (0–600 kGy) are presented in Fig. 7. A broad emission band was observed within the range of 400–600 nm. The PL spectral peak position of the irradiated PC films was redshifted compared with that of the unirradiated PC films (pristine). This is attributed to the formation of defects after irradiation or the partial release of hydrogen molecules, which resulted in the generation of carbon-rich clusters and a subsequent reduction in the optical bandgap energy [25]. Additionally, the PL intensity decreased as the irradiation dose increased. The PL peak intensity of the PC irradiated with 600 kGy decreased by 63.2% compared with that of the pristine samples (0 kGy). During the PL process, energy is transferred to the chromophore sites via UV excitation, and radiative recombination occurred in the thermalized electron–hole pairs o, thus resulting in fluorescence [51]. The decrease in the PL intensity may be associated with the formation of internal defects caused by radiation [52]. Radiation-induced disturbance in the internal structure of the PC resulted in the emergence of defect states, including chain scission and intermolecular crosslinking [53]. The formation of defects created a new radiative recombination level for electrons and holes in the PC [54].

Moreover, the fluorescence peak positions of all samples were concentrated at 470 nm. The relationship between the PL peak intensity value (y) and the irradiation dose (x) within the dose range of 20–600 kGy is shown in the upper right of Fig. 7. Linear regression fitting was performed, and the linear regression equation $y = -0.00695x + 6.32303$ was obtained, with a correlation coefficient of 0.965 (the standard error of this correlation coefficient is 1.72%). This correlation coefficient closely matches that of the Makrofol LT 6-4 PC film in the range of 150–950 kGy [25], thus demonstrating that the PC film maintained a favorable linear relationship in the dose capture range of 20–600 kGy.

3.8 Self-decay

The attenuation characteristics of the PL peak intensity in the irradiated PC film (300 kGy) within 60 days are shown in Fig. 8. Clearly, the PL peak intensity decreased continually

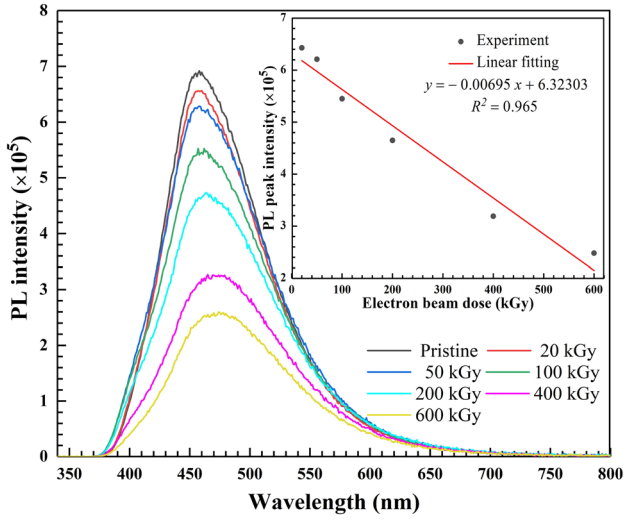

Fig. 7 (Color online) Emission spectrum and dose linear relationship of PC film

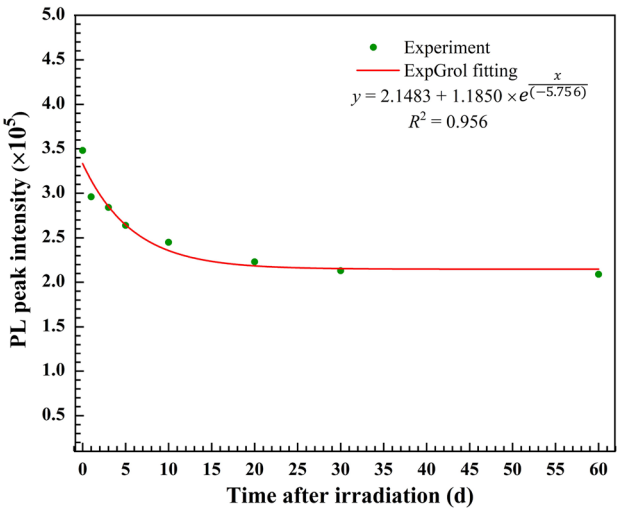

Fig. 8 (Color online) Attenuation characteristic of PL peak intensity of irradiated PC film within 60 days

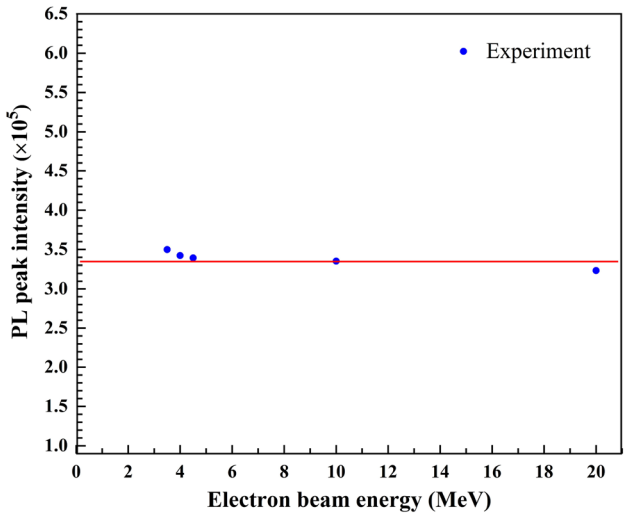

Fig. 9 (Color online) Electron energy response of PC irradiated film

with time. This may be due to the ambient temperature or other factors, thus resulting in a reduction in fluorescence centers inside the PC irradiated film. The results indicate a significant decrease in the PL peak intensity within the first 20 days after irradiation, with the peak intensity decreasing to 64% of its initial value. Subsequently, the declining trend became gentler over the following 40 days, with the peak intensity decreasing to 60% of the initial intensity within 60 days. Upon fitting with the ExpGro1 function, the following decay equation was obtained: $y = 2.1483+1.1850 \times e^{\frac{x}{-5.7560}}$. The correlation coefficient between the PL peak intensity (y) and time (x) was 0.956. Thus, the fitting function reflects the decline in the fluorescence intensity of the PC film to a certain extent. This phenomenon of fluorescence signal decay after irradiation is commonly observed in commercial thin-film dosimeters such as GD-300 RPL [42] and CTA dosimeters [55], and the decay characteristics depend on the material properties [36]. Considering the significant decay in the PL signal of this PC film in the initial days after irradiation, PL spectral testing should be conducted the soonest possible after irradiation, or the corresponding dose compensation should be performed based on the decay characteristic law.

3.9 Electron energy response

Figure 9 shows the PL peak intensity of the PC film irradiated by EBs of different energy levels (3.5, 4, 4.5, 10, and 20 MeV) under the same dose (100 kGy). The results show that the PL peak response values of the energy points were 3.499×10^5, 3.422×10^5, 3.39×10^5, 3.352×10^5, and 3.236×10^5, respectively. Using the PL peak intensity value at 10MeV as the normalized basis, the deviations of the PL peak intensity value at 3.5, 4, 4.5, and 20 MeV were +4.38%, +2.09%, +1.22%, and −3.46%, respectively. Based on a comparison with the energy response characteristics of GD-351 M RPL and LiF: Mg, Ti dosimeters [56], the signal intensity of the PC film exhibited a similar trend, although the amplitude of the change was smaller. This is because of the low density and small thickness of the PC film as well as the marginal difference in the electron energy response under irradiation with a high-energy EB (≥ 3.5 MeV).

4 Conclusion

In this study, the thickness applicability, preheating time, temperature and humidity dependence, in-batch uniformity, readout reproducibility, dose linearity, self-decay, and electron energy response of engineered PC films after EB irradiation were discussed based on PL spectrum analysis. Upon excitation with 320 nm UV light, the fluorescence peak of the PC film appeared at an emission wavelength of 470 nm. The results show that the optimal thickness for dose detection using the PC film was 0.3 mm and that the optimal fluorescence value can be obtained by preheating at 60 °C for 180 min. However, environmental factors such as temperature (during PL spectral testing) and humidity (both during irradiation and post-irradiation storage), can affect the PL intensity. At a low irradiation dose (100 kGy), the dose-response uniformity of the PC film was ideal. In the dose-capture range of 20–600 kGy, the PL spectral peak intensity of PC films showed favorable dose linearity ($R^2 = 0.965$) and readout reproducibility ($C_v \leq 8.6\%$). Additionally, when a PC film is used for radiation dose measurement, a PL spectrum test should be performed to prevent PL-signal decline after irradiation. Based on a comprehensive analysis of the aforementioned dosimetric parameters, this PC film can be proposed as a promising RPL material and demonstrates potential application in high-radiation dose detection.

Acknowledgements The authors thank the Science Compass experimental platform, China for providing the necessary fluorescence test conditions, and Xianghua Huada Biotechnology Co., Ltd., Hunan, China for providing irradiation conditions for the experiments.

Author Contributions All authors contributed to the study conception and design. Material preparation, data collection, and analysis were performed by Ke Wang, Xiong-Hui Fei, and Xiao-Dong Wang. The first draft of the manuscript was written by Ke Wang and all authors commented on previous versions of the manuscript. All authors read and approved the final manuscript.

Data Availability The data that support the findings of this study are openly available in Science Data Bank at https://cstr.cn/31253.11.sciencedb.j00186.00812 and https://www.doi.org/10.57760/sciencedb.j00186.00812.

Declarations

Conflict of interest The authors declare that they have no Conflict of interest.

References

1. L. Zhao, I.J. Das, Gafchromic EBT film dosimetry in proton beams. Phys. Med. Biol. **55**, N219–N301 (2010). https://doi.org/10.1088/0031-9155/55/10/N04
2. Z. Qin, Y.S. Hu, Y. Ma et al., Embedded structure fiber-optic radiation dosimeter for radiotherapy applications. Opt. Express **24**, 5172–5185 (2016). https://doi.org/10.1364/OE.24.005172
3. C.H. Li, Y.L. Zhang, R.C. Pang et al., Progress on standardization of electron beam dosimetry for radiation processing. Radiat. Phys. Chem. **42**, 823–826 (1993). https://doi.org/10.1016/0969-806X(93)90382-5
4. W.L. McLaughlin, J.M. Puhl, M. Murphy et al., Sunna dosimeter: an integrating photoluminescence film and reader system: work in progress. Radiat. Phys. Chem. **55**, 767–771 (1999). https://doi.org/10.1016/S0969-806X(99)00227-3
5. Z.L. Cai, X.N. Pan, H.T. Di et al., Dosimetry of ultrasoft x-rays (1.5 keV $Al_{K\alpha}$) using radiochromatic films and colour scanners. Phys. Med. Biol. **48**, 4111–4124 (2003). https://doi.org/10.1088/0031-9155/48/24/009
6. N. Wen, S.M. Lu, Y.J. Qin et al., Precise film dosimetry for stereotactic radiosurgery and stereotactic body radiotherapy quality assurance using Gafchromic ^{TM} EBT3 films. Radiat. Oncol. **11**(1), 132 (2016). https://doi.org/10.1186/s13014-016-0709-4
7. X. Sun, A. Banoushi, A. Mostofizadeh et al., Verification of Mason and Smythe equations for electrical treeing breakdown at the tip of charged particle tracks in ECE polycarbonate detectors. Radiat. Meas. **43**, 43–46 (2008). https://doi.org/10.1016/j.radmeas.2007.11.007
8. L.Z. Jiang, J.Y. Wu, K.X. Chen et al., Polymer waveguide Mach-Zehnder interferometer coated with dipolar polycarbonate for on-chip nitroaromatics detection. Sensor. Actuat. B-Chem. **305**, 127406 (2020). https://doi.org/10.1016/j.snb.2019.127406
9. S.A. Nouh, A. Mohamed, H.K. Marie, Proton-induced crosslinking of CR 6–2 polycarbonate. J. Appl. Polym. Sci. **112**, 2724–2731 (2009). https://doi.org/10.1002/app.29902
10. P.L. Forster, D.F. Parra, J. Kai et al., Effects of gamma radiation on the photoluminescence properties of polycarbonate matrices doped with terbium complex. Radiat. Phys. Chem. **79**, 347–349 (2010). https://doi.org/10.1016/j.radphyschem.2009.08.026
11. Y. Tao, M.Q. Li, X.Y. Liu et al., Dual-color plasmonic nanosensor for radiation dosimetry. Acs. Appl. Mater. Inter. **12**, 22499–22506 (2020). https://doi.org/10.1021/acsami.0c03001
12. A.M.S. Galante, A.L.C.H. Villavicencio, L.L. Campos, Preliminary investigations of several new dyed PMMA dosimeters. Radiat. Phys. Chem. **71**, 393–396 (2004). https://doi.org/10.1016/j.radphyschem.2004.05.038
13. W.L. McLaughlin, A. Miller, T. Preisinger et al., Plastic film materials for dosimetry of very large absorbed doses. Radiat. Phys. Chem. **25**, 729–748 (1985). https://doi.org/10.1016/0146-5724(85)90153-0
14. K. Cao, Y. Wang, Y. Wang, Effects of strain rate and temperature on the tension behavior of polycarbonate. Mater. Desi. **38**, 53–58 (2012). https://doi.org/10.1016/j.matdes.2012.02.007
15. C.Y. Xing, X. Zheng, L.Q. Xu et al., Toward an optically transparent, antielectrostatic, and robust polymer composite: morphology and properties of polycarbonate/ionic liquid composites. Ind. Eng. Chem. Res. **53**, 4304–4311 (2014). https://doi.org/10.1021/ie404096b
16. L.K. Massey, *The Effect of Sterilization Methods on Plastics and Elastomers*, 2nd edn. (ScienceDirect, New York, 2004), pp.41–61
17. Y.M. Sun, Z.Y. Zhu, Z.G. Wang et al., The damage process induced by swift heavy ion in polycarbonate. Nucl. Instrum. Meth. B. **212**, 211–215 (2003). https://doi.org/10.1016/S0168-583X(03)01735-X
18. E.S. Araujo, H.J. Khoury, S.V. Silveira, Effects of gamma-irradiation on some properties of durolon polycarbonate. Radiat. Phys. Chem. **53**, 79–84 (1998). https://doi.org/10.1016/S0969-806X(97)00300-9
19. Z.Y. Zhu, Y.M. Sun, C.L. Liu et al., Chemical modifications of polymer films induced by high energy heavy ions. Nucl. Instrum. Meth. B. **193**, 271–277 (2002). https://doi.org/10.1016/S0168-583X(02)00773-5
20. S.A. Nouh, A. Mohamed, T.M. Hegazy et al., Modification induced by alpha particle irradiation in Makrofol polycarbonate. J. Appl. Polym. Sci. **109**, 3447–3451 (2008). https://doi.org/10.1002/app.28469
21. L. Wang, W.H. Chung, D. Fink et al., On the dyeing of ion tracks in polymers. Nucl. Instrum. Meth. B. **108**, 377–384 (1999). https://doi.org/10.1016/0168-583X(95)01161-7
22. S.L. Guo, J. Drach, P.B. Price et al., Calibration of Tuffak polycarbonate track detector for identification of relativistic nuclei. Radiat. Meas. **9**, 183–188 (1984). https://doi.org/10.1016/0735-245X(84)90183-2
23. Z.H. Wei, L.Q. Wei, H. Gang et al., Comparisons of dosimetric properties between GD-300 series of radiophotoluminescent glass detectors and GR-200 series of thermoluminescent detectors. Nucl. Sci. Tech. **18**, 362–365 (2007). https://doi.org/10.1016/S1001-8042(08)60009-3
24. M.F. Zaki, S.I. Elkalashy, T.S. Soliman, A comparative study of the structural, optical, and morphological properties of different types of Makrofol polycarbonate. Polym. Bull. **79**, 10841–10863 (2022). https://doi.org/10.1007/s00289-021-04011-2
25. A.M. Abdul-Kader, M.F. Zaki, R.M. Radwan et al., Influence of gamma irradiation on physical and chemical properties of Makrofol (NTD) material. Radiat. Phys. Chem. **151**, 12–18 (2018). https://doi.org/10.1016/j.radphyschem.2018.05.010
26. T. Posavec, S. Nepal, S.V. Dordevic, Low temperature photoluminescence in some common polymers. Mater. Perf. Charact. **7**, 178–185 (2018). https://doi.org/10.1520/MPC20170138
27. A.M.S. Galante, L.L. Campos, Mapping radiation fields in containers for industrial γ-irradiation using polycarbonate dosimeters. Appl. Radiat. Isotopes. **70**, 1264–1266 (2012). https://doi.org/10.1016/j.apradiso.2011.12.046
28. V. Resta, G. Quarta, L. Calcagnile et al., Raman and Photoluminescence spectroscopy of polycarbonate matrices irradiated with different energy $^{28}Si^{+}$ ions. Vacuum **116**, 82–89 (2015). https://doi.org/10.1016/j.vacuum.2015.03.005
29. M. Kattan, Y. Daher, H. Alkassiri, A high-dose dosimeter-based polyvinyl chloride dyed with malachite green. Radiat. Phys. Chem. **76**, 1195–1199 (2007). https://doi.org/10.1016/j.radphyschem.2006.12.004
30. R.M. Bhata, B.S. Tomarb, Evaluation of an indigenously manufactured Garfilm-EM-250 μm thick polyester film as a dosimeter for high-dose applications. Radiat. Phys. Chem. **77**, 64–73 (2008). https://doi.org/10.1016/j.radphyschem.2007.02.071
31. A. Mejri, K. Farah, H. Eleuch, Application of commercial glass in gamma radiation processing. Radiat. Meas. **43**, 1372–1376 (2008). https://doi.org/10.1016/j.radmeas.2008.05.010
32. Z.Q. Liu, X.S. Yi, A.M. Cunha et al., Key properties to understand the performance of polycarbonate reprocessed by injection molding. J. Appl. Polym. Sci. **77**, 1393–1400 (2000)
33. Z.Y. Xiao, L. Zhang, R. Hansel et al., Temperature dependence of the photostimulated luminescence in, KCl: Eu^{2+}. Nucl. Instrum. Meth. B. **58**, 182–184 (2014). https://doi.org/10.1016/j.nimb.2013.09.031
34. R.J. Yang, S.P. Xu, W.J. Jiang et al., Dosimetric comparison between helical tomotherapy and step-and-shoot intensity modulated radiation therapy for endometrial carcinoma, 2nd edn. (Chinese Journal of Cancer, Beiing, 2009), pp. 1121-6

35. J. Li, C.X. Zhang, Q. Tang et al., Synthesis, photoluminescence, thermoluminescence and dosimetry properties of novel phosphor $Zn(BO_2)_2$:Tb. J. Phys. Chem. Solids **68**, 143–147 (2007). https://doi.org/10.1016/j.jpcs.2006.09.021
36. M. Lin, H.Z. Li, Y.D. Chen et al., Thin film alanine-PE dosimeter for electron beam transfer dosimetry. Radiat. Phys. Chem. **73**, 280–286 (2005). https://doi.org/10.1016/j.radphyschem.2004.10.004
37. Y.H. Wang, Q. Li, L. Chen et al., Simulation study of the dose and energy responses of FNTD personal neutron dosimetry. Nucl. Sci. Tech. **30**, 32 (2019). https://doi.org/10.1007/s41365-019-0546-x
38. J. Jin, J.X. Liu, X.Q. Wang et al., Effect of color center absorption on temperature dependence of radiation-induced attenuation in optical fibers at near infrared wavelengths. J. Lightwave Technol. **31**, 839–845 (2013). https://doi.org/10.1109/JLT.2012.2235173
39. D. Zoul, M. Koplová, M. Zimina et al., Study of chemical processes in irradiated polycarbonate in the context of its applicability for integrating dosimetry of high doses. Radiat. Phys. Chem. **177**, 109203 (2020). https://doi.org/10.1016/j.radphyschem.2020.109203
40. E. Kosobrodova, A. Kondyurin, W. Chrzanowski et al., Optical properties and oxidation of carbonized and cross-linked structures formed in polycarbonate by plasma immersion ion implantation. Nucl. Instrum. Meth. B. **329**, 52–63 (2014). https://doi.org/10.1016/j.nimb.2014.03.010
41. S. Lu, X. Gao, C.Y. Hu et al., Heavy metal release from irradiated LDPE/nanometal composite films into food simulants. Food Packag. Shelf Life **26**, 100571 (2020). https://doi.org/10.1016/j.fpsl.2020.100571
42. W.H. Zhuo, W.Q. Liu, G. Huang et al., Radiation dosimetry characteristics of GD-300 series radiation photoluminescent glass dosimeters. Atom. Energy Sci. Tech. **12**, 1120–1124 (2008). (**in Chinese**)
43. Y.L. Liu, M.H. Huo, S.Z. Ruan et al., EPR dosimetric properties of different window glasses. Nucl. Instrum. Meth. B. **443**, 5–14 (2019). https://doi.org/10.1016/j.nimb.2019.01.022
44. J. Castrellon-Uribe, M. Güizado-Rodríguez, R. Espíndola-Rivera, Photoluminescence analysis of a polythiophene derivative: concentration and temperature effects. Opt. Mater. **58**, 93–101 (2016). https://doi.org/10.1016/j.optmat.2016.03.049
45. C.H. Li, Y.L. Zhang, R.C. Pang et al., Progress on standardization of electron beam dosimetry for radiation processing. Radiat. Phys. Chem. **42**, 823–826 (1993). https://doi.org/10.1016/0969-806X(93)90382-5
46. V.H. Ritz, A note on Mylar film dosimetry. Radiat. Res. Chem. **15**, 460–466 (1961). https://doi.org/10.2307/3571289
47. D.T. Turner, *Polyethylene terephthalate*, 2nd edn. software (Chemical Week, New York, 1973), pp. 137-164
48. H. Levine, W.L. McLaughlin, A. Miller, Temperature and humidity effects on the gamma-ray response and stability of plastic and dyed plastic dosimeters. Radiat. Phys. Chem. **14**, 551–574 (1979). https://doi.org/10.1016/0146-5724(79)90091-8
49. N.B. Liu, M.H. Li, X.Y. Li et al., PET-based biodistribution and radiation dosimetry of epidermal growth factor receptor–selective tracer 11C-PD153035 in humans. J. Nucl. Med. **50**, 303–308 (2009). https://doi.org/10.2967/jnumed.108.056556
50. N. Vitaly, Accuracy considerations in EPR dosimetry. Appl. Radiat. Isotopes. **52**, 1039–1050 (2000). https://doi.org/10.1016/S0969-8043(00)00052-X
51. M.F. Zaki, W.A. Ghaly, H.S. El-Bahkiry, Photoluminescence, optical band gap and surface wettability of some polymeric track detectors modified by electron beam. Surf. Coat. Tech. **275**, 363–368 (2015). https://doi.org/10.1016/j.surfcoat.2015.04.041
52. X.H. Zhang, L. Shao, J. Li et al., Radiation damage in nanostructured materials. Prog. Mater Sci. **96**, 217–321 (2018). https://doi.org/10.1016/j.pmatsci.2018.03.002
53. M.F. Zaki, E.K. Elmaghraby, Photoluminescence of gamma-radiation induced defect on poly allyl diglycol carbonates. J. Lumin. **132**, 119–121 (2012). https://doi.org/10.1016/j.jlumin.2011.08.001
54. J.H. Yang, L. Shi, L.W. Wang et al., Non-radiative carrier recombination enhanced by two-level process: a first-principles study. Sci. Rep-UK **6**, 21712 (2016). https://doi.org/10.1038/srep21712
55. F. Abdel-Rehim, A.A. Abdel-Fattah, S. Ebrahim et al., Improvement of the CTA dosimetric properties by the selection of readout wavelenght and the calculation of the spectrophotmetric quantity. Appl. Radiat. Isotopes. **47**, 247–258 (1996). https://doi.org/10.1016/0969-8043(95)00233-2
56. K. Eljka, S. Liliana, B. Igor et al., Photon dosimetry methods outside the target volume in radiation therapy: Optically stimulated luminescence (OSL), thermoluminescence (TL) and radiophotoluminescence (RPL) dosimetry. Radiat. Meas. **57**, 9–18 (2013). https://doi.org/10.1016/j.radmeas.2013.03.004